Available online at www.worldscientificnews.com

World Scientific News

WSN 56 (2016) 217-228 EISSN 2392-2192

The impact of Cu alloy on auxiliary and invisible options of splash kept CdS slims

Mohammed A. Kadhim

Physic Department, Science College, Karbala University, Iraq

E-mail address: malmengushi@gmail.com

ABSTRACT

Cadmium Sulfide and copper alloyed $Cd_{1-x}S$ Cu_x slims have been set up by the spray pyrolysis technique. The optical gap crevices at unadulterated and doped Cadmium Sulfide were observed to be shifted from (2.34 to 2.45) eV with increment x from (0 to 0.1). The X-beam diffraction (XRD) investigation uncovered that slims were polycrystalline and showed two phases cubic and hexagonal structure with increasing the hexagonal phase with increment Cu ratio.

***Keywords*:** CdS; spray pyrolysis; optical properties; Cu concentration

1. INTRODUCTION

CdS films are generally utilized as a window layer as a part of heterojunction sun oriented cells attributable to their wide band crevice and the simplicity with which the material can be set up by ease strategies. CdS has straight band gap of 2.4 eV, which falls in the noticeable range at room temperature [1]. CdS can exists in two phases, hexagonal with a = 4.1370 Å and c = 6.7144 Å[2] and cubic with a = 5.8330 Å [3], the hexagonal (wurtzite) Cadmium Sulfide films are ideal for sun oriented cell useful because of their unbelievable dependability in photoelectric transformation and heterogeneous photo catalysis. Nonetheless, it is difficult to acquire the film having a hexagonal structure as it was [4].

2. EXPERIMENTAL PROCEDURE

Prior to deposit films, It has been cleaned glass substrates in With cleaner solution, distilled water, followed by alcohol using an ultrasonic bath.

$Cd_{1-x}SCu_x$ films were prepared by using an aqueous solution which contained $CdCl_2$, $CuCl_2$ and thiourea. In the solution, the Cd+Cu to S ratio was maintained at 1:1.5. The excess sulfur was used to maintain stoichiometry in the films. The high substrate temperature causes loss of sulfur during deposition. The cadmium concentration in the solution was (1-x)*1M. The Cu concentration in the solution was (x)*1M (where x = 0, 0.05 and 0.10). The ionic arrangement was showered onto hot glass substrates held at 673K utilizing compacted air as the transporter gas. The spray rate employed was 3 mL per min.

X-ray diffraction (XRD) pattern of the CdS film deposited on corning glass substrate is recorded by SHIMADZU XRD-600 X-ray diffract meter (Cu_α radiation λ = 0.154 nm) in 2θ range from 20° to 60°. The interplaner distanced d_{hkl} for different planes is measured using Bragg law [5]

$$2d \sin \theta = m \lambda \qquad \text{……...1}$$

where d is the interference distance, Θ is Brrag's angle, m is order level and λ is the incident wave length

While the average crystallite size (b) estimated by Scherrer's formula [6]:

$$b = \frac{0.89\,\lambda}{\Delta(2\theta).\cos(\theta)} \qquad \text{……..2}$$

where: Δ is full width half maximum.

The thickness of arranged films was about 500 nm By Nicholson measured overlap. Permeability in the wavelength range have been recorded optical absorption spectra, at room temperature, (400 - 1100 nm) using the Optima SP-3000 UV-Vis laboratory. The absorption factor (α) of CdS pure and doped copper thin membrane permeability measurements of the light spectrum using the formula[7]:

$$\alpha = \frac{1}{d} \ln\left(\frac{1}{T}\right) \qquad \text{…… 3}$$

As d is the density of thin slims, and **T** is the transmittance intensity. The energy gap and optical constants the account as a function of various Cu focuses.

3. RESULTS AND DISCUSSION

Fig. (1) demonstration the X-ray deviation patterns for pure and doped CdS films with various doping ratio with Cu (0, 5 and 10 %) this figure indicate all films have polycrystalline structure and have a good identically with standard peaks for booth hexagonal and cubic CdS at increment the hexagonal phase with increasing Cu ratio. In addition we can

also see from table (1) a decreasing in d_{hkl} with increasing Cu content i.e., slightly shift in 2θ to higher value (as shown in the two dimensional intensity, Figure 2) because the size of Cu ion (which have been inserted into lattice) less than for Cd ion.

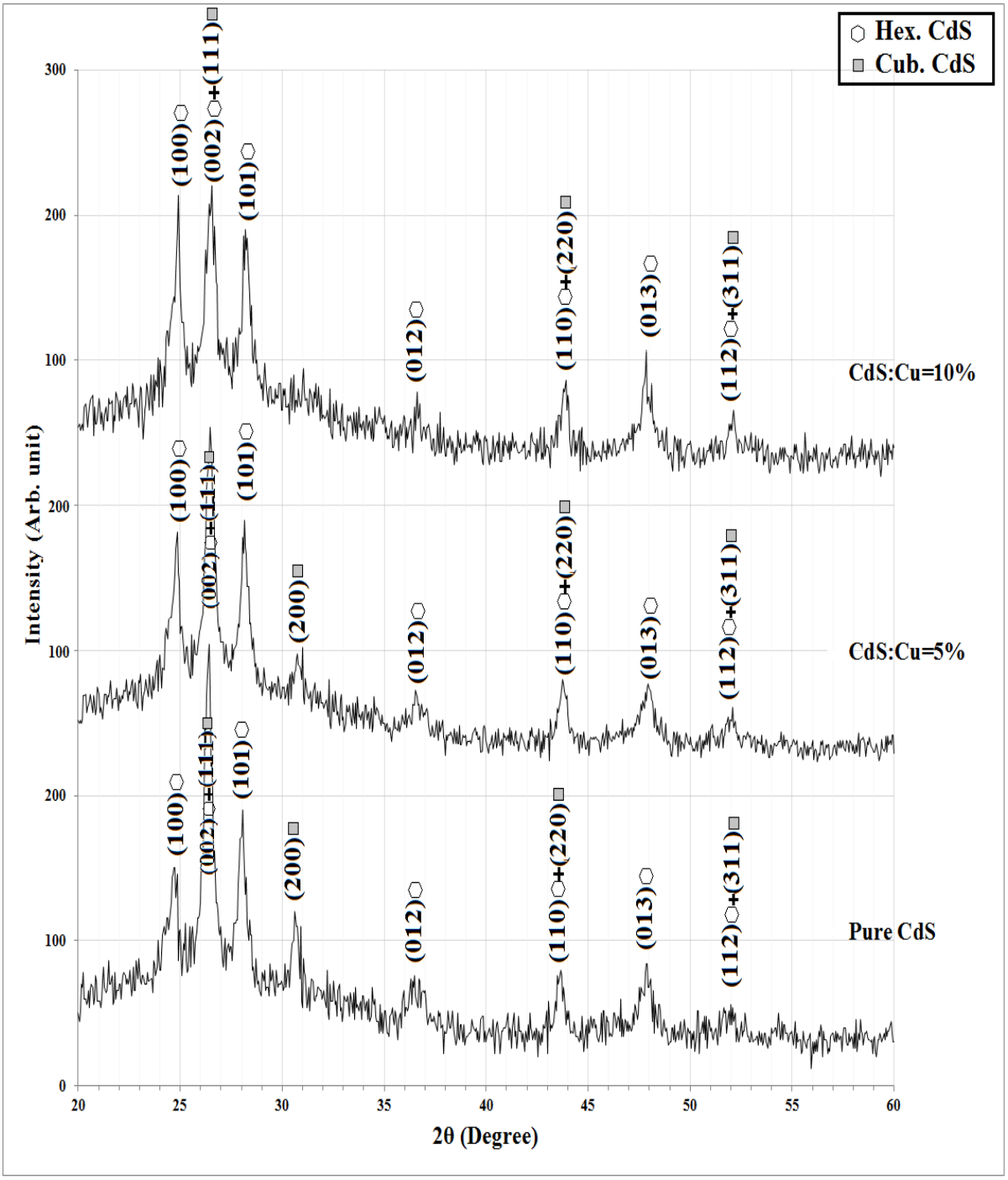

Fig. 1. X-ray deviation style for $Cd_{1-x}S\ Cu_x$ with different Cu ratio (0, 5 and 10 %)

Table 1. Structural parameters: Inter-planar spacing, crystalline size of depo-sited pure and doped CdS films at different Cu doping ratio (0, 5 and 10) %.

Cu %	2θ (Deg.)	FWHM (Deg.)	d_{hkl} Exp.(Å)	G.S (nm)	d_{hkl} Std.(Å)	hkl	phase	card No.
0	24.7084	0.6872	3.6003	11.8	3.5827	(100)	Hex. CdS	96-901-1664
	26.4363	0.4754	3.3688	17.2	3.3572	(002)	Hex. CdS	96-901-1664
					3.3677	(111)	Cub. CdS	96-900-0109
	28.0778	0.4385	3.1754	18.7	3.1609	(101)	Hex. CdS	96-901-1664
	30.6263	0.5330	2.9168	15.5	2.9165	(200)	Cub. CdS	96-900-0109
	36.5011	1.2099	2.4597	6.9	2.4498	(012)	Hex. CdS	96-901-1664
	43.6717	0.7962	2.0710	10.7	2.0685	(110)	Hex. CdS	96-901-1664
					2.0623	(220)	Cub. CdS	96-900-0109
	47.8618	0.9942	1.8990	8.7	1.8982	(013)	Hex. CdS	96-901-1664
	52.0086	0.9651	1.7569	9.2	1.7611	(112)	Hex. CdS	96-901-1664
					1.7587	(311)	Cub. CdS	96-900-0109
5	24.8812	0.3771	3.5757	21.6	3.5827	(100)	Hex. CdS	96-901-1664
	26.4795	0.5211	3.3634	15.7	3.3572	(002)	Hex. CdS	96-901-1664
					3.3677	(111)	Cub. CdS	96-900-0109
	28.1641	0.4002	3.1659	20.5	3.1609	(101)	Hex. CdS	96-901-1664
	30.7559	0.7722	2.9048	10.7	2.9165	(200)	Cub. CdS	96-900-0109
	36.5443	0.7930	2.4569	10.5	2.4498	(012)	Hex. CdS	96-901-1664
	43.7581	0.4863	2.0671	17.6	2.0685	(110)	Hex. CdS	96-901-1664
					2.0623	(220)	Cub. CdS	96-900-0109
	47.9482	0.7351	1.8958	11.8	1.8982	(013)	Hex. CdS	96-901-1664
	52.0518	0.5313	1.7556	16.6	1.7611	(112)	Hex. CdS	96-901-1664
					1.7587	(311)	Cub. CdS	96-900-0109
10	24.9244	0.4191	3.5696	19.4	3.5827	(100)	Hex. CdS	96-901-1664
	26.5659	0.5911	3.3526	13.8	3.3572	(002)	Hex. CdS	96-901-1664
					3.3677	(111)	Cub. CdS	96-900-0109
	28.2073	0.4653	3.1611	17.6	3.1609	(101)	Hex. CdS	96-901-1664
	36.6307	0.2991	2.4513	28.0	2.4498	(012)	Hex. CdS	96-901-1664
	43.9309	0.4634	2.0594	18.5	2.0685	(110)	Hex. CdS	96-901-1664

					2.0623	(220)	Cub. CdS	96-900-0109
	47.9050	0.5687	1.8974	15.3	1.8982	(013)	Hex. CdS	96-901-1664
	52.1382	0.4815	1.7529	18.4	1.7611	(112)	Hex. CdS	96-901-1664
					1.7587	(311)	Cub. CdS	96-900-0109

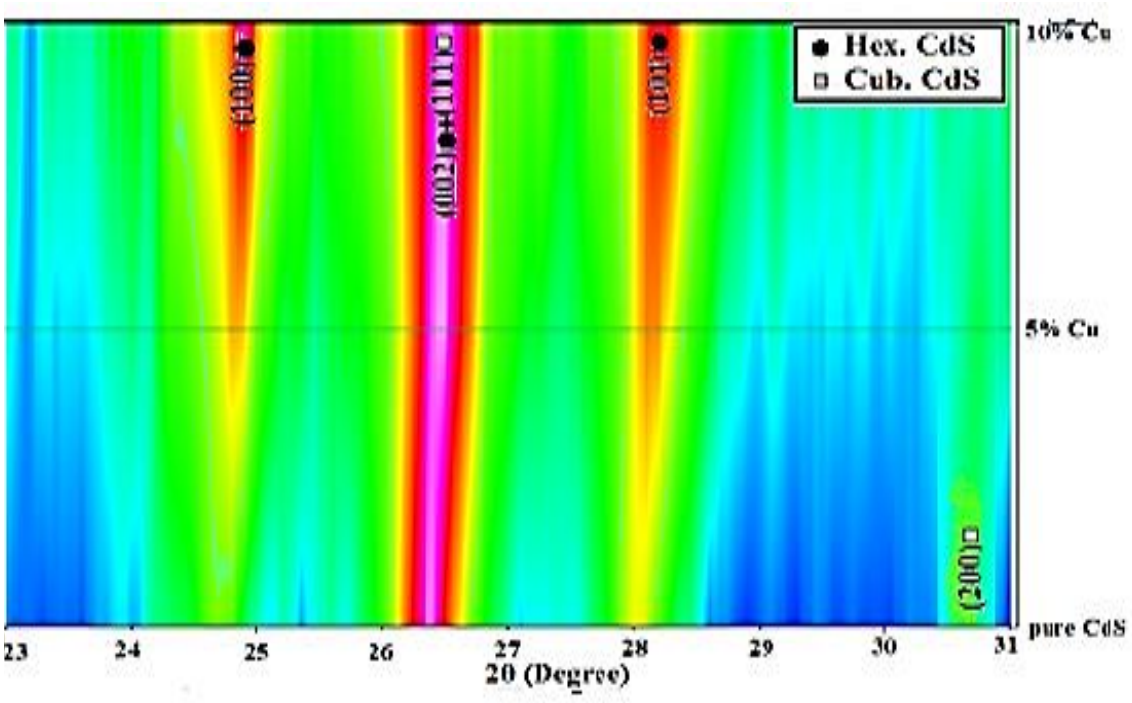

Fig. 2. Two dimensional X-ray deviation styles intensities for $Cd_{1-x}S\ Cu_x$ with different Cu ratio (0, 5 and 10 %)

Table (2) demonstrations a decrement in lattice constants for Hexagonal and cubic phases which have been observed in XRD patterns.

Table 2. Lattice constants for Hexagonal and cubic observed phases in XRD patterns.

Cu:Cd %	Cubic	Hex	
	a (nm)	a (nm)	c (nm)
0	5.8349	4.1573	6.7376
5	5.8256	4.1289	6.7268
10	5.8069	4.1218	6.7052

Optical measurements for deposited $Cd_{1-x}S\ Cu_x$ prone to the glass substrate with various doping focuses are done in the wave length range (420–1100) nanometer as deposition (RT). Figure (3) demonstrations the room temperature (as deposition transmittance spectra for

samples doped with various Cu focuses. This figure shows that the transmittance increments with expanding of wavelength (λ). Then again the transmittance diminishes with the expansion of Cu fixation

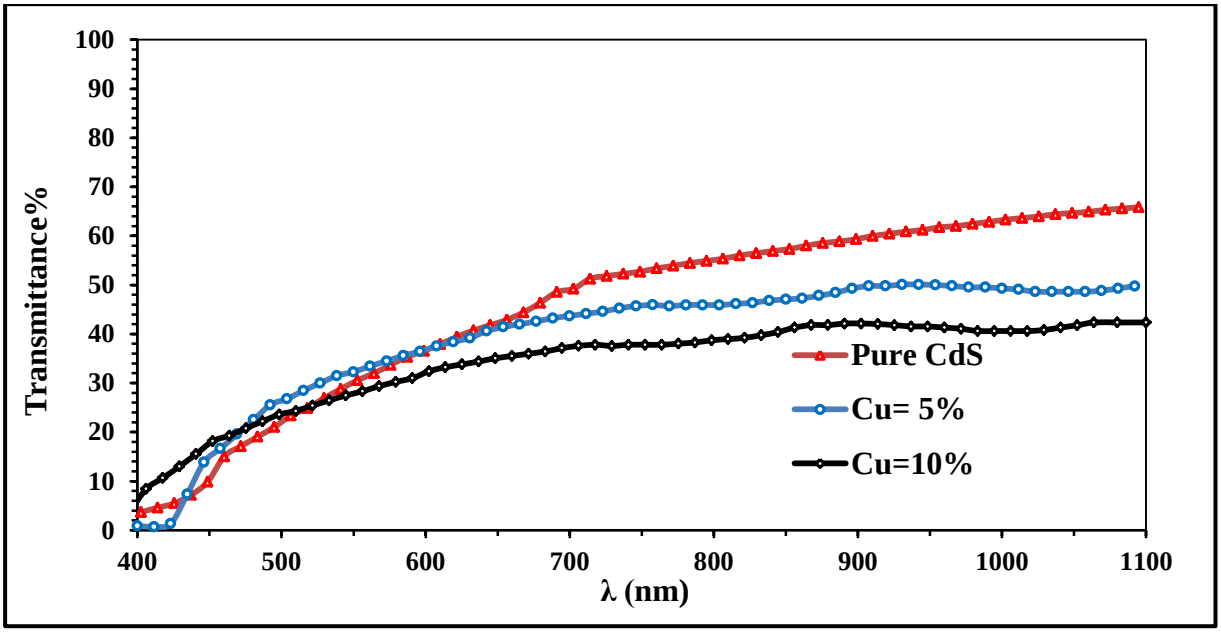

Fig. 3. Transmittance variation with the wavelength for pure and doped CdS films with Cu.

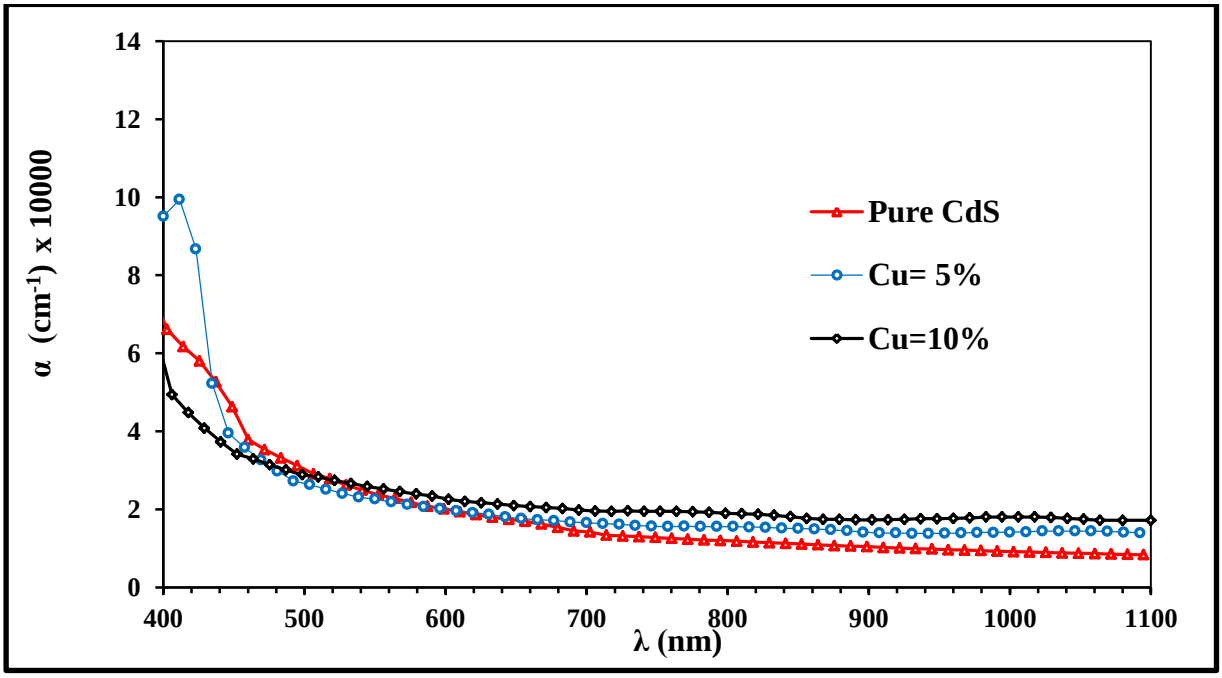

Fig. 4. Variety of assimilation factor with the wavelength for refined and alloy CdS films with Cu.

Figs. (4) Explain the contrast of assimilation factor with wavelength for $Cd_{1-x}S\ Cu_x$ films on glass substrate with diverse doping focuses. All spectrums represent ingestion factor example in all saved immaculate and doped slim CdS movies diminish with expanding of wavelength (λ) from 420 to 1100 nm. Then again the ingestion coefficient increments with the expansion of Cu focus.

The optical vitality hole values (E_g^{opt}) for slims CdS films on glass have been controlled by utilizing Tauc condition. [8].

$$\alpha h\upsilon = A\left(h\upsilon - E_g\right)^r$$

As hυ is the photon vitality, Eg is the optical band hole energy, A is contrarily corresponding to amorphousity and r is utilized to discover the kind of the optical transition by plotting the relations $(\alpha h\upsilon)^{1/2}$, $(\alpha h\upsilon)^{1/3}$, $(\alpha h\upsilon)^{2/3}$, and $(\alpha h\upsilon)^2$ versus photon vitality (hυ). The vitality gap (Eg) is then dictated by the extrapolation of the direct divide at $(\alpha h\upsilon)2 = 0$. It is found that the connection for r = 1/2 yields direct reliance part at which the ingestion coefficient $\alpha \geq 10^4 cm^{-1}$, that explain $Cd_{1-x}SCu_x$ films have allow to straight transition. This result will be the subject of agreement at result had shown by the previous researches.

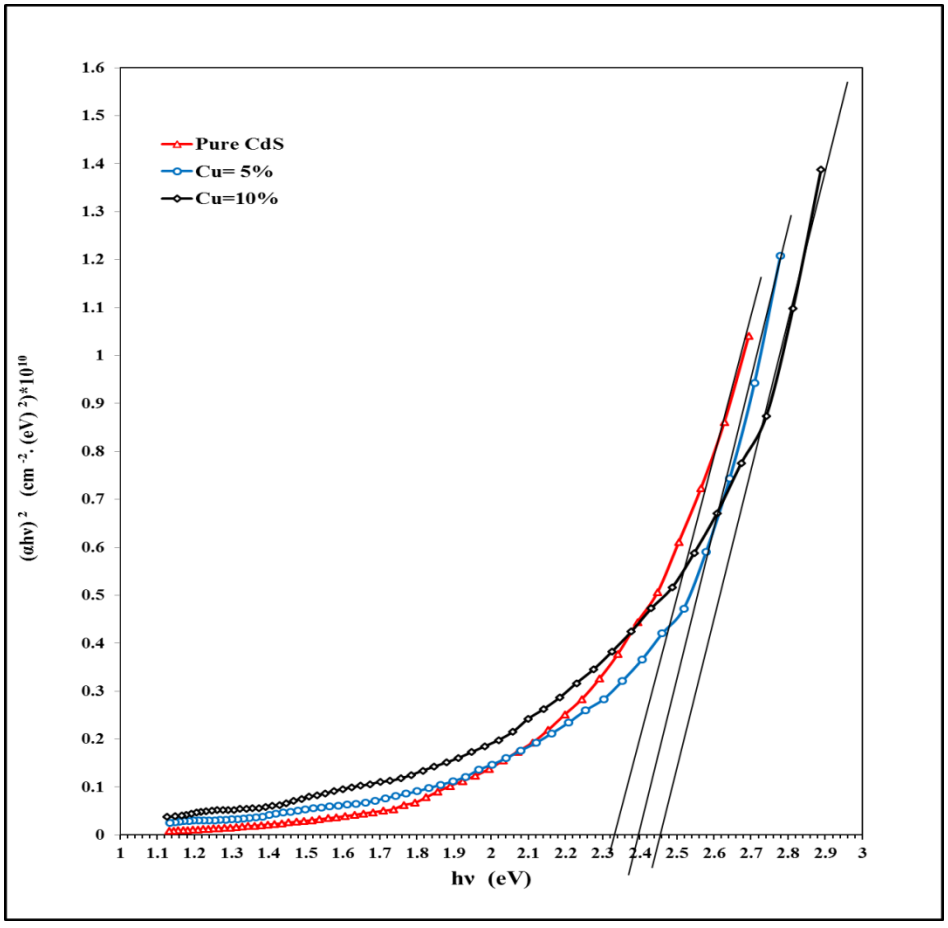

Fig. 5. The variety of $(\alpha h\upsilon)^2$ versus photon energy (hυ) for for fresh and doped CdS films with Cu.

The variety of $(\alpha h\upsilon)^2$ as a component of photon vitality for immaculate and Cu doped slim CdS films at different Cu concentration have been plotted in Figure(5). This case display that the expanding of Cu focus from(0 to 10)% leads to increase the energy gap from approximately 2.34 eV to 2.45 eV. This may be ascribed to decrease lattice constants.[9]

It is critical to decide the optical constants of flimsy movies, for example, refractive file (n), termination factor (k), and the genuine (ε_r) and fanciful (ε_i) parts at insulation steady.

Figure (6) demonstrates the variety at eradication factor with wavelength at various Cu alloy proportion. The eradication factor consists mostly at retention factor; therefore, the conduct from it is comparative for ingestion factor i.e. the expanding of termination coefficient with expanding photon vitality in light of the fact that the assimilation is expanded.

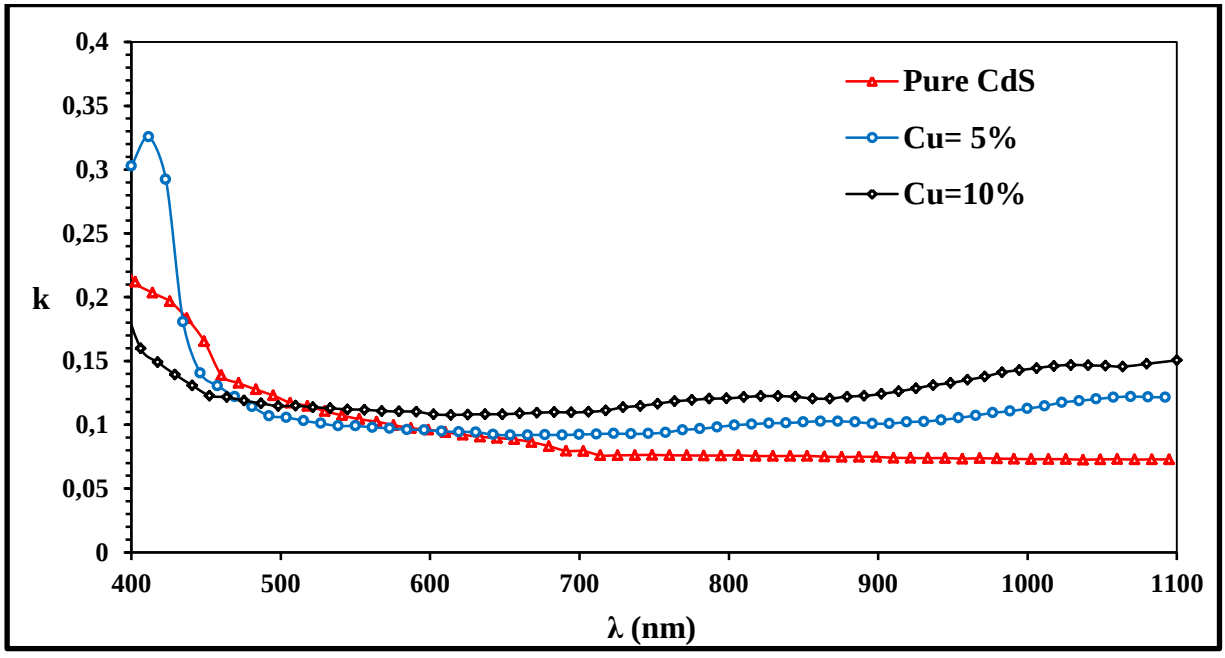

Fig. 6. Annihilation coefficient versus wavelength for unadulterated and doped CdS slims with Cu.

The list of refraction at refresh and Cu doped thin CdS slims were assessed in the reflectance (R) information utilizing the connection[10]:

$$n = \sqrt{\frac{4R}{(1-R)^2} - k^2} - \frac{R+1}{R-1}$$

The variety at the refractive record opposite wavelength at the reach 400-1000 nm, as deposited CdS slims on glass at distinctive Cu alloy focuses films have been appeared in Figure (7). Obviously through assume the refractive file all at all increment at expanding for alloy focus with Cu.

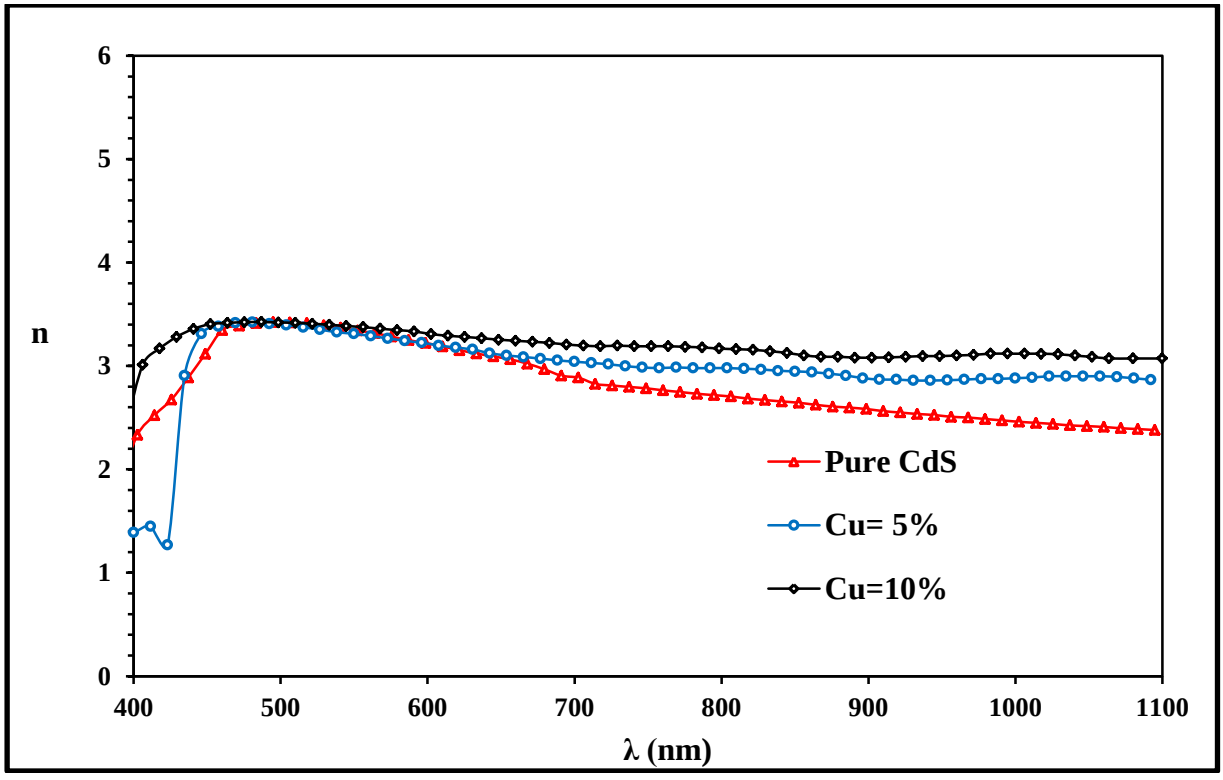

Fig. 7. Divergence of refractive index with the wavelength for pure and doped CdS films with Cu.

The genuine and fanciful parts of dielectric consistent were assessed utilizing the equations [11]:

$$\varepsilon_r = n^2 - k^2$$

$$\varepsilon_i = 2nk$$

The variety from genuine and fanciful throughout the dielectric constants values opposite wavelength have been appeared in Figures (8 & 9) until kept unadulterated and Cu alloyed slight CdS films on glass with various doping focuses. Their worths are diminished at wavelength more than 500 nm.The variety from the insulation consistent relies on upon the estimation at refractive record. By differentiation, the insulation misfortune consists predominantly at annihilation factors valuable which are identified with the variety of retention.

Chart (1) demonstrates the optical constants for saved immaculate and Cu doped slender CdS movies on glass with various doping focuses (0 , 5 & 10) % at λ = 800 nm furthermore, the scan crevice valuable for these readied tests. This Chat outlines that the estimations of α, k, n, ε_r, ε_i and E_g increment at expanding Cu alloy focuses, while the conduct of T is inverse i.e., diminish with expanding Cu doping fixations.

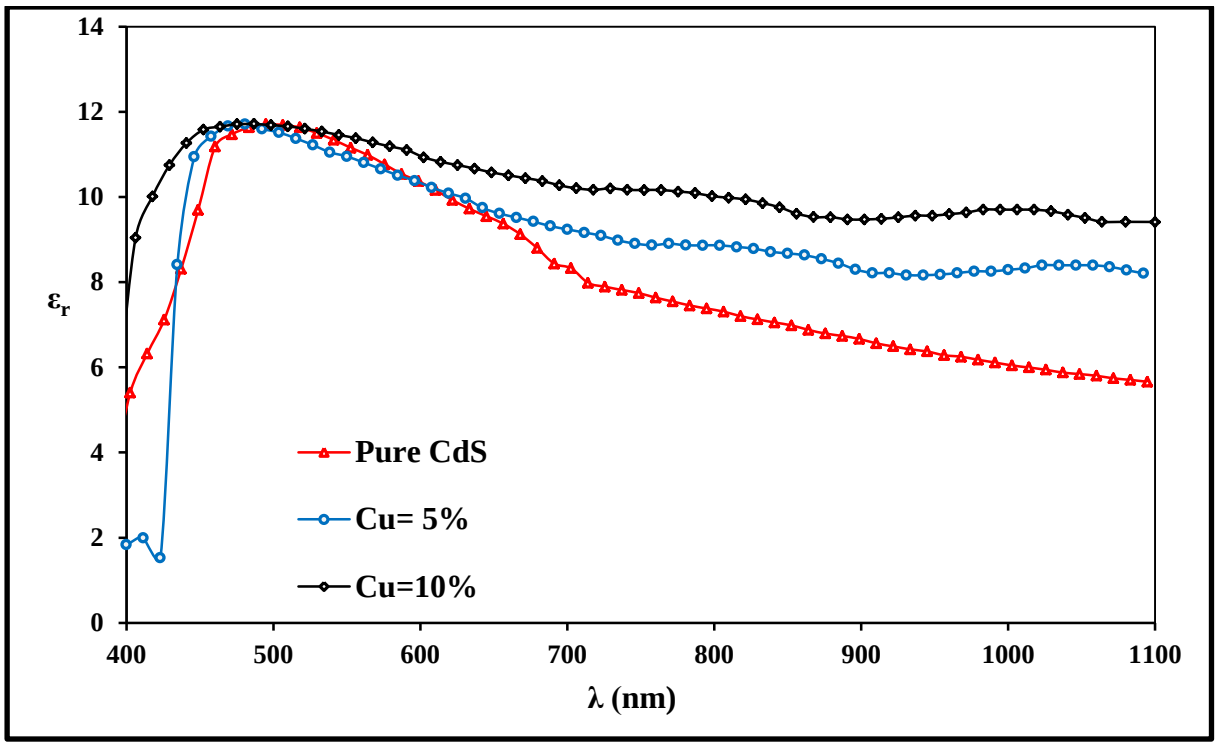

Fig. 8. The variety of ε_r with the wave length for immaculate and doped CdS films with Cu.

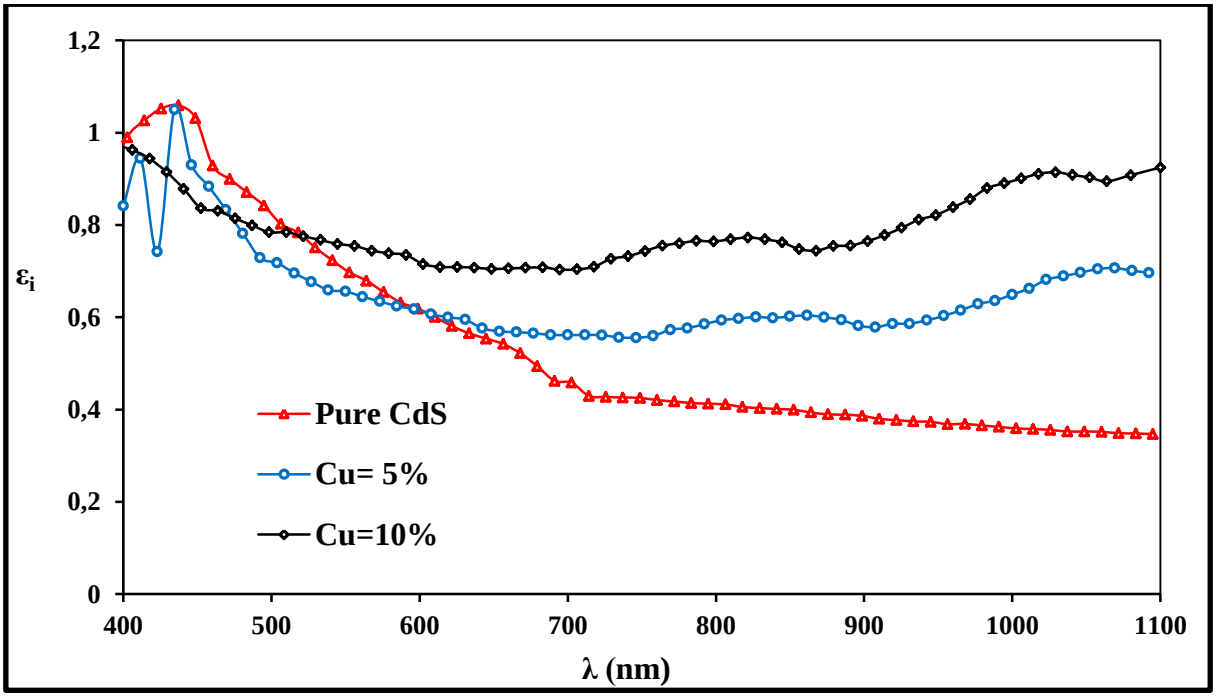

Fig. 9. The variation of ε_i with the wave length for pure and doped CdS films with Cu.

Chart 1. The optical parameters at λ = 800 nm and E_g for immaculate and doped CdS films at various Cu doping focuses.

Cu%	T%	α (cm^{-1})	K	n	ε_r	ε_i	Eg (eV)
0	54.91	11992	0.076	2.718	7.381	0.413	2.34
5	45.92	15567	0.098	2.979	8.866	0.585	2.40
10	38.73	18976	0.121	3.168	10.021	0.764	2.45

4. CONCLUSIONS

Structural and optical properties of $Cd_{1-x}SCu_x$ thin films set up by spray pyrolysis statement method have been considered as a component of diverse Cu alloy fixations. The result of this investigation may be summarized as follows:

- XRD indicates that all $Cd_{1-x}SCu_x$ films have polycrystalline structure and have booth hexagonal and cubic CdS phases and increment the hexagonal phase with rise Cu ratio.
- Decreasing in d_{hkl} with increasing Cu content i.e., slightly shift in 2θ to higher because the size of Cu ion less than for Cd ion. i.e decreasing in lattice constants.
- The optical permeability increment at expanding wavelength at that time diminishes at expanding Cu inlay(graft) focuses.
- Vitality whole (E_g) increments from 2.34 eV to 2.45 eV with the expansion of Cu doping focuses from 0 to 10% because of the decrement in cross section constants.
- Constants values optical (α, k, n, εr and εi) are increment at expanding Cu alloy fixations.

References

[1] S. Kar and S. Chaudhuri, *Met. Org. Nano-Metal Chem.* 36 (2006) 289-312.

[2] Xu Y. N., Ching W. Y., Electronic, optical, and structural properties of some wurtzite crystals, *Physical Review B*, 48 (1993) 4335-4351.

[3] B. Skinner, Unit-cell edges of natural and synthetic sphalerites Locality: synthetic, *American Mineralogist*, 46 (1961) 1399-1411.

[4] J. Ximello-Quiebras, G. Contreras-Puente, J. Aguilar-Hernandez, G. Santana Rodriguez and A. Arias-Carbajal Readigos, *Sol. Energ. Mater. Sol Cells*, 82 (2004) 263.

[5] Fundamentals of the Physics of Solids, Vol. I Structure and Dynamics Translated by Attila, 1999, Piroth, Vol. 242, p. 261.

[6] B. Warren, X-ray Diffraction, Addison-Wesley Publishing Company, (1969), p: 253.

[7] Z. Rizwan, A. Zakaria, M. Ghazali, A. Jafari, F. Ud Din, and R. Zamiri, *Int. J. Mol. Sci.*, 12 (2011) 1293.

[8] J. Tauc, Amorphous and Liquid Semiconductors, Plenum Press, London and New York (1974).

[9] S. M. Sze and Kwok K. Ng, Physics of Semiconductor Devices. Third Edition, A John Wiley & Sons, Jnc., Publication, (2006), p. 60.

[10] S. Aksoy, Y. Caglar, S. Ilican, and M. Caglar, *Optica Applicata*, V. XL, N.1 (2010) 7.

[11] L. Kazmerski, Polycrystalline and Amorphous Thin Films and Devices, Academic Press (1980).

(Received 28 September 2016; accepted 14 October 2016)